Solid State Sciences 13 (2011) 534–538

Contents lists available at ScienceDirect

Solid State Sciences

journal homepage: www.elsevier.com/locate/ssscie

The oxidation behaviors of a ZrB_2–SiC–ZrC ceramic

Zhi Wang, Zhanjun Wu*, Guodong Shi

School of Aeronautics and Astronautics, Faculty of Vehicle Engineering and Mechanics, State Key Laboratory of Structural Analysis for Industrial Equipment, Dalian University of Technology, Dalian 116024, PR China

ARTICLE INFO

Article history:
Received 13 July 2010
Received in revised form
2 December 2010
Accepted 9 December 2010
Available online 16 December 2010

Keywords:
ZrB_2-based ceramic
Microstucture
Oxidation kinetics

ABSTRACT

The specimen of a ZrB_2–SiC–ZrC ceramic was heated by the electrical resistance heating and the temperature of the specimen increased linearly to 1750 °C within 40s. ZrB_2–SiC–ZrC ceramic was oxidized in air for 30 min and the microstructure of oxide layer was investigated and discussed. The analysis of the SEM observations combined with EDS confirmed that the layered structure consisted of: (1) a SiO_2-rich glass layer; (2) a thin layer of ZrO_2–SiO_2; (3) a layer of ZrO_2 and/or ZrB_2 from which SiC had been depleted; (4) unaffected ZrB_2–SiC–ZrC ceramic. Furthermore, the oxidation kinetics of ZrB_2–SiC–ZrC ceramic was investigated in detail.

1. Introduction

Ceramic compounds of refractory borides, carbides and nitrides, such as ZrB_2, HfB_2, TaC, ZrC, HfC and HfN, belong to a group of materials known as ultrahigh temperature ceramics (UHTCs) [1–4]. Interest in UHTCs has increased significantly in recent years because of the drive to produce a thermal protection system and other components for hypersonic aerospace vehicles, reusable launch vehicles, or rocket engines [5]. Among the UHTCs, zirconium diboride (ZrB_2) based ceramics have attracted much attention because of their unique combination of relatively low density, good electrical and thermal conductivity, high hardness, high melting temperature and thermal shock resistance as well as excellent mechanical and chemical stability at high temperatures [6]. Historic studies implied that phase pure diborides could not be pressureless sintered to full density due to strong covalent bond and low self-diffusion as well as the hexagonal crystal structure that allowed for anisotropic grain growth and entrapped porosity (i.e., coarsening is more favorable than densification) [7,8]. The research about densification is driven by aerospace applications because the low densification causes the reduction in combination properties of ZrB_2 ceramics. Without sintering additives, ZrB_2 ceramics have only been densified by hot-pressing at above 2000 °C with pressures of 20–30 MPa, or at reduced temperatures (1790–1840 °C) with much higher pressures (800–1500 MPa) [9]. Although addition of silicon carbide (SiC) can improve the densification of ZrB_2–SiC ceramics, high sintering temperature of ≥1850 °C is still necessary [10]. Our previous works have revealed that in situ synthesis processing at relatively low temperature (1700 °C) is a good method for producing ZrB_2–20 vol.%SiC–6 vol.%ZrC (ZrB_2–SiC–ZrC) ceramics with homogenous microstructure and excellent mechanical properties [11]. The ZrB_2–SiC–ZrC ceramic is a leading candidate as potential materials for thermal protection structures in the form of rigid surfaces in areas of ultrahigh working temperature. The oxidation behaviors of ZrB_2–SiC–ZrC ceramic is a major issue for the potential application. There are many methods available for the investigation of the oxidation behaviors of UHTCs, such as the oxyacetylene torch [12], the plasma torch [13], the high temperature furnace [14] and so on. Unsatisfactorily, these methods have many disadvantages, for instance, the disadvantages of the oxyacetylene torch, the plasma torch and the high temperature furnace are bigger temperature error, high cost and low heating rate, respectively [12–14].

In the present work, The ZrB_2–SiC–ZrC ceramic was heated by electrical resistance heating. The main purpose of this paper is to report the oxidation behaviors of the ZrB_2–SiC–ZrC ceramic. The microstucture of the ZrB_2–SiC–ZrC ceramic after oxidation was analyzed and the oxidation kinetics of the ZrB_2–SiC–ZrC ceramic was investigated in detail.

2. Experimental

The preparation procedure of ZrB_2–20 vol.%SiC–6 vol.%ZrC (ZrB_2–SiC–ZrC) ceramic was described elsewhere[11]. Bulk of

* Corresponding author. Tel./fax: +86 411 84706791.
E-mail address: wzdlut@dlut.edu.cn (Z. Wu).

1293-2558/$ – see front matter © 2010 Elsevier Masson SAS. All rights reserved.
doi:10.1016/j.solidstatesciences.2010.12.022

ZrB_2–20 vol.%SiC–6.05 vol.%ZrC ceramic was fabricated by in situ hot-pressing reaction synthesis. Sample was heated at 10 °C min^{-1} from room temperature to 1650 °C and then held at this temperature for 60 min in argon atmosphere. The application of pressure began at 1500 °C and gradually increased to 30 MPa before the temperature reached a value of 1650 °C. After sintering, the furnace was cooled to room temperature under flowing argon. The bulk density of the ZrB_2–SiC–ZrC ceramic was measured using the Archimedes' technique with deionized water as the immersing medium. The relative density was determined by dividing the bulk density by the theoretical density. The phase composition was determined by X-ray diffraction (XRD; Rigaku, Dmax-rb, CuKa = 1.5418 Å and a graphite monochromator). The schematic diagram of home-made oxidation device with power of 50 kW is shown in Fig. 1A, which was used for the oxidation behaviors of ZrB_2–SiC–ZrC ceramic. Specimen coupons were cut by mechanical cutting into 3 by 4 by 36 mm and each specimen was ground and polished with diamond slurries down to a 1 μm finish. The edges of all the specimens were chamfered to minimize the effect of stress concentration due to machining flaws. The specimen was fixed in Cu electrode and the temperature of the specimen center was measured by multi-wavelength pyrometer with measurement range of 1000–2500 °C. Finite element analysis (FEA) was used to simulate the temperature distribution in the specimen. The room temperature thermal expansion coefficient, thermal diffusivity, thermal conductivity and specific heat, were 6.81×10^{-6} K^{-1}, 0.27 cm^2/s, 135 W/m K and 827J/kg·K, respectively. The electrical resistivity of the specimen was 15 μΩ cm^{-1} and the thermal conductivity of air was 0.0241 W/m K. These thermophysical properties of a ZrB_2–SiC–ZrC ceramic with increasing temperature up 1800 °C have been submitted other journal. The voltage for two ends of specimen was maintained at 3 V and the temperature was controlled by the system program. The schematic diagram of electronic weighing device during oxidation is shown in Fig. 1B. The isothermal oxidation of the specimens was carried out in static air at a constant temperature of 1750 ± 15 °C. The mass of the specimen was determined on an electronic balance; its accuracy was ±0.1 mg. The weight change/unit area (w) of the specimen was calculated by:

$$w = \frac{\frac{m_0 - m_t}{m_0}}{A} \quad (1)$$

where m_0 and m_t are the weight of the specimen before oxidation and after oxidation time of t s, respectively, A is the surface area of the specimen. The microstructural observations of specimen were carried out by scanning electron microscopy (SEM, 20 kV, FEI Sirion, Holland) along with energy dispersive spectroscopy (EDS, EDAX Inc) for chemical analysis.

3. Results and discussion

3.1. Microstructure

An XRD spectrum obtained from the polished surface of the ZrB_2–SiC–ZrC ceramic is shown in Fig. 2A. Apparently, the phase analysis indicated the predominant phases for the ZrB_2–SiC–ZrC ceramic were ZrB_2, SiC and a small quantity of ZrC. No other phases were observed, which indicated that the reaction was completed. Fig. 2B shows the polished surface of ZrB_2–SiC–ZrC ceramic. It could be found by EDS analysis (not shown here) that the microstructure of ZrB_2–SiC–ZrC ceramic was characterized by the grey ZrB_2, dark SiC and light ZrC. The theoretical density was calculated according to the rule of mixtures based on the densities of 6.09, 3.21, and 6.44 g/cm^3 for ZrB_2, SiC, and ZrC, respectively [15]. The theoretical density of ZrB_2 containing 20 vol.%SiC plus 6 vol.%ZrC was calculated to be 5.54 g/cm^3. Based on this bulk density of 5.40 g/cm^3, the relative density of the ZrB_2–SiC–ZrC ceramic was calculated to be >97.5% that was higher than 95% of the ZrB_2–SiC composite by reactive hot-pressing at temperature of 1650 °C[16], which was attribute to high reactive temperature. The porosity was not considered to have a significant effect on the oxidation behavior because ZrB_2–SiC–ZrC ceramic had high relative density.

The surface of specimen after electrical resistance heating showed symmetric distribution of morphologies as shown in Fig. 3A, which revealed that during the heating period the macro-scale temperature field was not uniform at the two ends and middle of the specimen, namely, the temperature of middle part of the specimen was higher than the two ends. This phenomena can be observed in many metallic specimen heated by electrical resistance heating. Furthermore, the temperature field of the micro-scale at the same distance away from the electrode seems not uniform because the electrical conductivities of ZrB_2, SiC and ZrC are different, however, the temperature field of the micro-scale at the same distance away from the electrode was thought uniform because the SiC and ZrC in the three-dimensional space are not continuous, the thermal conductivities of ZrB_2, SiC and ZrC are high and the different phases are close contact. The temperature distribution in the specimen was simulated by Finite element analysis (FEA) as shown in Fig. 3B. The features of the electrical resistance heating and rectangular geometry of the specimen resulted in non-uniform heating, with the temperature of middle part of the specimen higher than the ends. The FEA indicated that middle part of the maximum and uniform temperature accounted for about 20% of whole specimen, which was favorable for the oxidation investigation of the specimen because the maximum temperature field had larger uniform region. The simulated maximum temperature of 1739 °C was considerable to the

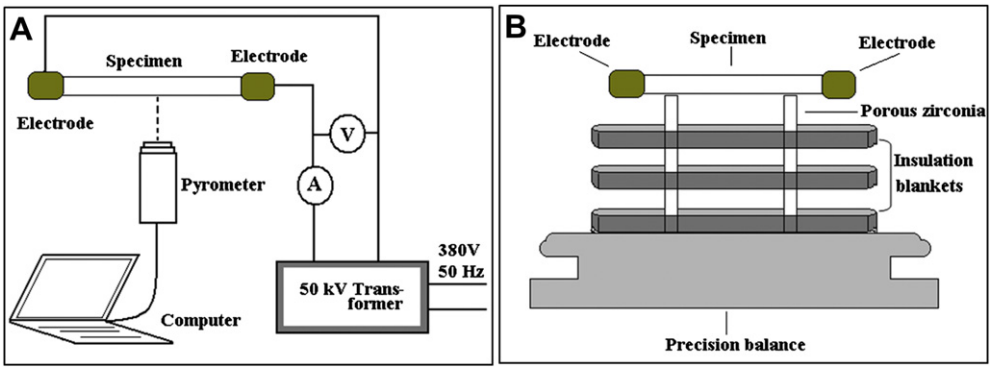

Fig. 1. Schematic diagram of oxidation device (A) and electronic weighing device (B).

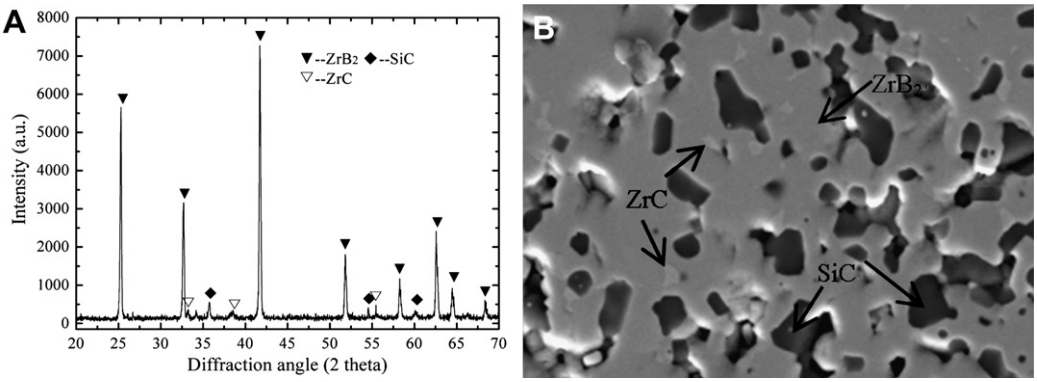

Fig. 2. XRD spectrum (A) and the microstructure (B) of polished surface of ZrB_2–SiC–ZrC ceramic.

measured temperature of 1750 °C, which revealed that the simulated temperature distribution in the specimen was convincible. The surface of the specimen was oxidized when the specimen was exposed to high temperature air [17]. For example, ZrB_2 was oxidized to ZrO_2 and B_2O_3 at above 800 °C; SiC was oxidized to SiO_2 and CO_2 at above 900 °C; ZrC was oxidized to ZrO_2 and CO_2 at above 450 °C. So, the specimen was heated at 1750 °C for 30 min and the main expected chemical reactions were as follows:

$$ZrB_2(s) + 5/2O_2 \rightarrow ZrO_2(s) + B_2O_3(l) \quad (2)$$

$$B_2O_3(l) \rightarrow B_2O_3(g) \quad (3)$$

$$SiC(s) + 3/2O_2 \rightarrow SiO_2(l) + CO(g) \quad (4)$$

$$ZrC(s) + 3/2O_2 \rightarrow ZrO_2(s) + CO(g) \quad (5)$$

$$SiO_2(l) + B_2O_3(l) \rightarrow SiO_2 \cdot B_2O_3(l) \quad (6)$$

Fig. 4 shows the surface microstructure of the specimen oxidized at the temperature of 1750 °C. A large amount of the glass formed on the surface of the specimen and the extensive bubble formation was observed on the glass. The EDS analysis (not shown here) confirmed that the glass was the SiO_2-rich layer because the glass phase mainly contained O and Si without other elements. This SiO_2-rich layer is expected to contain some B_2O_3 during heating based on either incomplete evaporation of the B_2O_3 by Reaction (3) or the continued production of B_2O_3 beneath the outer scale by Reaction (2) [17]. The formation of the large bubbles was attributed presumably to the escape of the gaseous products inside the external forming glass [18]. The bubbles tended to burst when the vapor pressure in the bubbles exceeded the sum of the ambient pressure and the tensile force of the SiO_2-rich layer. The growth of large bubbles beneath the external layer often caused local spalling of the SiO_2-rich layer layer, which resulted in the revelation of the ZrO_2–SiO_2 layer that was confirmed by EDS analysis, namely, a large number of small white ZrO_2 particles that were covered with the thin SiO_2-rich glass were also detected. Such microstructure of the ZrO_2–SiO_2 layer on the surface could be due to the solidification of a liquid zirconia [19].

The microstructures of the cross-section of the specimen oxidized for 30 min are shown in Fig. 5. The analysis of the SEM observations combined with EDS demonstrated that the layered structure consisted of: (1) a SiO_2-rich glass layer; (2) a thin layer of ZrO_2–SiO_2; (3) a layer of ZrO_2 and/or ZrB_2 from which SiC had been partially depleted; (4) unaffected ZrB_2–SiC–ZrC ceramic. Such layered structure was similar to the microstructure reported for ZrB_2–30 vol.%SiC ceramics exposed to air at high temperature [16–18]. The formation of a SiO_2-rich glass layer was very effective in limiting the inward diffusion of oxygen into the inner bulk, thus enhancing the resistance to oxidation. The thickness of the oxidation layers of the specimen oxidized at 1750 °C for 30 min was equivalent to that of ZrB_2–30 vol.%SiC ceramics oxidized at 1400 °C for 30 min [17], which was attributed presumably to the high volatility of the SiO_2-rich glass layer on the surface of ZrB_2–SiC–ZrC ceramic at 1750 °C because the boiling point of borosilicate glass was about 1700 °C [20]. The volume expansion upon conversion of ZrB_2 and ZrC to ZrO_2 was 13.0% and 36.5%, respectively, based on density calculations [17]. The addition of ZrC phase was also favorable to enhance oxidation resistance because the pores from

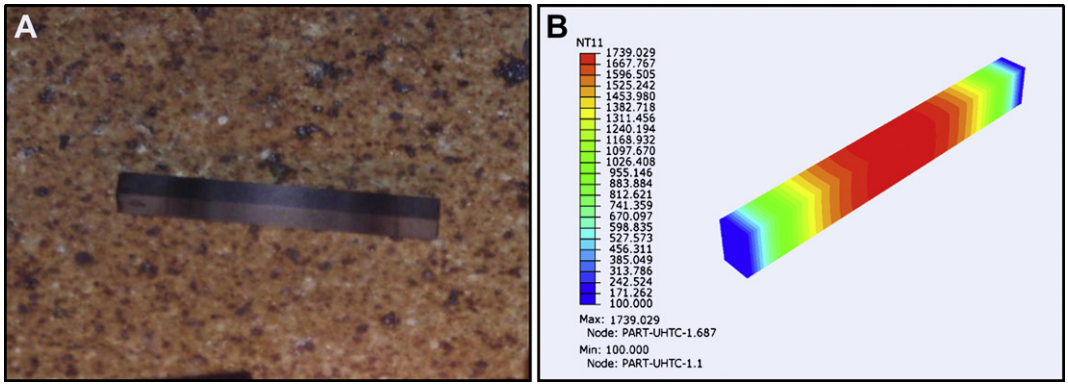

Fig. 3. Macrograph (A) of specimen after electrical resistance heating and temperature distribution (B) during the heating period.

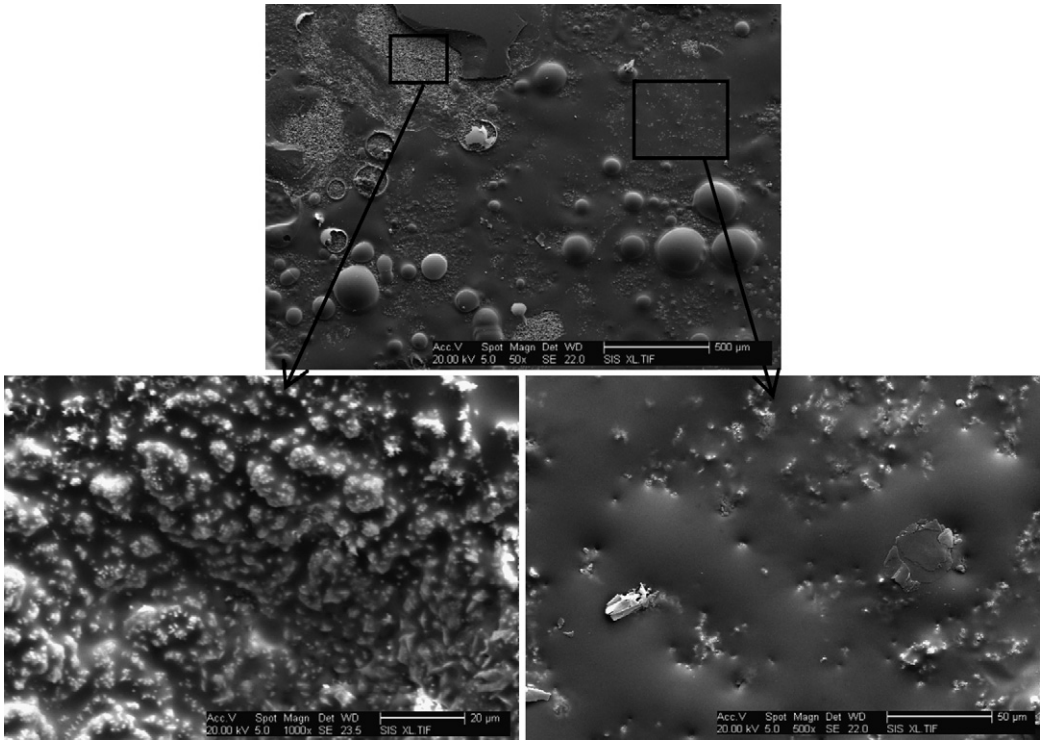

Fig. 4. The surface microstructure of the specimen oxidized at the temperature of 1750 °C.

which SiC was depleted were filled due to the volume expansion, although a small quantity of pores was still observed as shown in Fig. 5.

In this paper, the whole surface was considered as surface area of the specimen. In order to further investigate the oxidation mechanism of the ZrB_2–SiC–ZrC composite, the weight change/unit area (w) of the specimen with increasing oxidation time is shown in Fig. 6. The automatic fitting of the weight change/unit area and the oxidation time was carried out by Origin system, which revealed that the weight change/unit area increased as the oxidation time increased with parabolic behavior. The parabolic oxidation kinetics of ZrB_2–SiC–ZrC ceramic could be explained by the solid-state diffusion [21,22]. The continuous oxide layer separated the substrate from the oxygen gas. The oxidation reaction could proceed only by the solid-state diffusion of the oxygen through the previously formed oxide layer. In the initial stage, the chemisorption nuclei formed on the surface of the specimen and the weight change/unit area due to oxidation was controlled by the chemical reaction. After the formation of continuous oxide layer the weight change/unit area was controlled by the diffusion rate of the oxygen through oxide layer. Based on the Fick's first law [21,22], the diffusion flux, J, of oxygen through oxide layer:

$$J = -D_0 A \frac{\partial C}{\partial X} \tag{7}$$

$$J \cong -D_0 A \frac{\Delta C}{X} \tag{8}$$

where A is the oxidized surface area of the specimen, ΔC is the concentration difference between gas/oxide layer interface and oxide layer/substrate interface, X is the thickness of the oxide layer. After the formation of continuous oxide layer a steady state was obtained and the diffusion flux, J, of oxygen through oxide layer was equal to the quantity of oxygen consumed by oxide layer growth in unit time dt [23,24]:

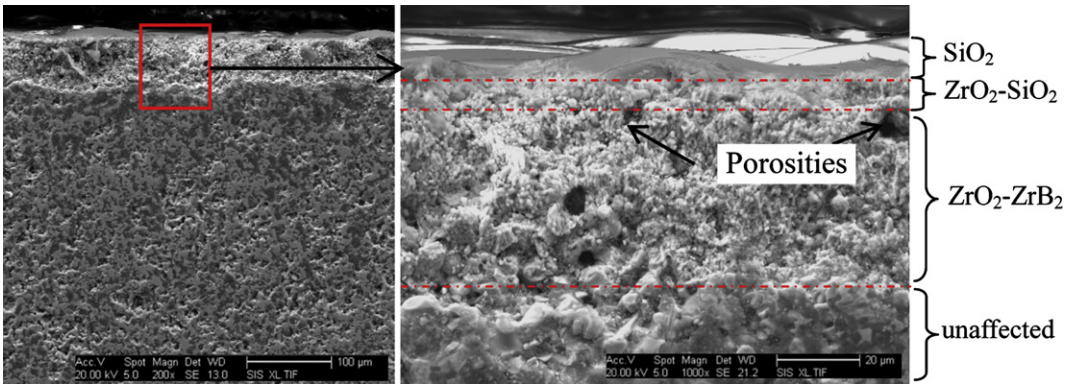

Fig. 5. The microstructures of the cross-section of the specimen oxidized for 30 min.

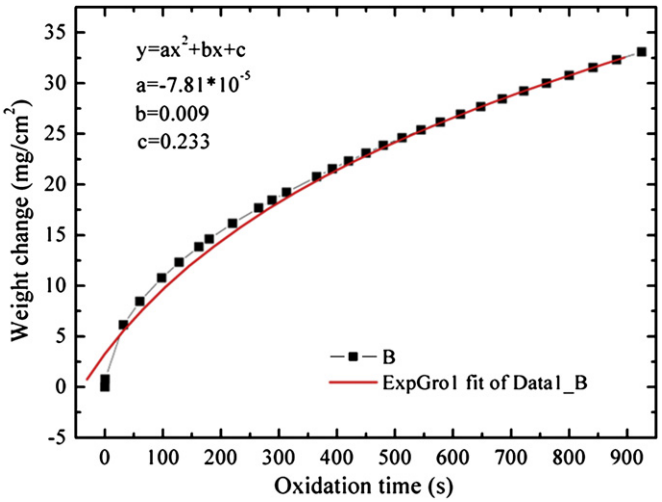

Fig. 6. The weight change/unit area (w) of the specimen with increasing oxidation time.

$$-D_0 A\frac{\Delta C}{X} = Ad_0\frac{dX}{dt} \tag{9}$$

where dX is the thickness of oxide layer growth, d_0 is the quantity of oxygen consumed by oxide layer growth. To integrate Eq. (9), the thickness of the oxide layer X was obtained as:

$$X^2 = \frac{2\Delta C D_0}{d_0}t \tag{10}$$

ΔC, D_0 and d_0 in steady state are constants; Eq. (10) was transformed as following:

$$X^2 = kt \tag{11}$$

Based on theoretical derivation and experimental results, the oxidation reaction of the ZrB_2–SiC–ZrC ceramic was mainly controlled by diffusion rate of oxygen through oxide layer because oxidation kinetics obeyed the parabolic law, which is consistent with the conclusions reported in the literatures [25–27].

4. Conclusion

The ZrB_2–SiC–ZrC ceramic was rapidly heated by electrical resistance heating. The analysis of the SEM observations combined with EDS demonstrated that the layered structure consisted of: (1) a SiO_2-rich glass layer; (2) a thin layer of ZrO_2–SiO_2; (3) a layer of ZrO_2 and/or ZrB_2 from which SiC had been partially depleted; (4) unaffected ZrB_2–SiC–ZrC ceramic. Based on theoretical derivation and experimental results, the oxidation reaction of the ZrB_2–SiC–ZrC ceramic was controlled by diffusion rate of oxygen through oxide layer because oxidation kinetics obeyed the parabolic law.

Acknowledgments

This work was supported by “China Postdoctoral Science Foundation Funded Project and the Fundamental Research Funds for the Central Universities (3014-852001)” and the National Natural Science Foundation of China (51002019 and 91016024).

References

[1] L. Weng, X.H. Zhang, W.B. Han, J.C. Han, Fabrication and evaluation on thermal stability of hafnium diboride matrix composite at severe oxidation condition, Int. J. Refract. Met. Hard Mater. 27 (2009) 711–717.
[2] S.H. Meng, G.Q. Liu, J. An, S.L. Sun, Effects of different additives on microstructure and crack resistance for an ultra-high temperature ceramic, Int. J. Refract. Met. Hard Mater. 27 (2009) 813–816.
[3] D.J. Chen, L. Xu, X.H. Zhang, B.X. Ma, P. Hu, Preparation of ZrB_2 based hybrid composites reinforced with SiC whiskers and SiC particles by hot-pressing, Int. J. Refract. Met. Hard Mater. 27 (2009) 792–795.
[4] Y. Zhao, L.J. Wang, G.J. Zhang, W. Jiang, L.D. Chen, Effect of holding time and pressure on properties of ZrB_2–SiC composite fabricated by the spark plasma sintering reactive synthesis method, Int. J. Refract. Met. Hard Mater. 27 (2009) 177–180.
[5] X.Y. Li, X.H. Zhang, J.C. Han, C.Q. Hong, W.B. Han, A technique for ultrahigh temperature oxidation studies of ZrB_2–SiC, Mater. Lett. 62 (2008) 2848–2850.
[6] Q. Liu, W.B. Han, X.H. Zhang, S. Wang, J.C. Han, Microstructure and mechanical properties of ZrB_2–SiC composites, Mater. Lett. 63 (2009) 1323–1325.
[7] F.Y. Yang, X.H. Zhang, J.C. Han, S.Y. Du, Mechanical properties of short carbon fiber reinforced ZrB_2–SiC ceramic matrix composites, Mater. Lett. 62 (2008) 2925–2927.
[8] X.H. Zhang, L. Xu, S.Y. Du, J.C. Han, P. Hu, W.B. Han, Fabrication and mechanical properties of ZrB_2–SiC_w ceramic matrix composite, Mater. Lett. 62 (2008) 1058–1060.
[9] W.G. Fahrenholtz, G.E. Hilmas, I.G. Talmy, J.A. Zaykoski, Refractory diborides of zirconium and hafnium, J. Am. Ceram. Soc. 90 (5) (2007) 1347–1364.
[10] X.H. Zhang, Z. Wang, X. Sun, W.B. Han, C.Q. Hong, Effect of graphite flake on the mechanical properties of hot pressed ZrB_2–SiC ceramics, Mater. Lett. 62 (2008) 4360–4362.
[11] Q. Qu, J.C. Han, W.B. Han, X.H. Zhang, C.Q. Hong, In situ synthesis mechanism and characterization of ZrB_2–ZrC–SiC ultra high-temperature ceramics, Mater. Chem. Phys. 110 (2008) 216–221.
[12] S.F. Tang, J.Y. Deng, S.J. Wang, W.C. Liu, K. Yang, Ablation behaviors of ultra-high temperature ceramic composites, Mater. Sci. Eng. A 465 (2007) 1–7.
[13] R. Savino, M.D.S. Fumo, L. Silvestroni, D. Sciti, Arc-jet testing on HfB_2 and HfC-based ultra-high temperature ceramic materials, J. Eur. Ceram. Soc. 28 (2008) 1899–1907.
[14] J.C. Han, P. Hu, X.H. Zhang, S.H. Meng, Oxidation behavior of zirconium diboride-silicon carbide at 1800 °C, Scr. Mater. 57 (2007) 825–828.
[15] X.H. Zhang, Q. Qu, J.C. Han, W.B. Han, C.Q. Hong, Microstructural features and mechanical properties of ZrB_2–SiC–ZrC composites fabricated by hot pressing and reactive hot pressing, Scr. Mater. 59 (2008) 753–756.
[16] A.L. Chamberlain, W.G. Fahrenholtz, G.E. Hilmas, Low-temperature densification of zirconium diboride ceramics by reactive hot pressing, J. Am. Ceram. Soc. 89 (12) (2006) 3638–3645.
[17] A. Rezaie, W.G. Fahrenholtz, G.E. Hilmas, Evolution of structure during the oxidation of zirconium diboride-silicon carbide in air up to 1500 °C, J. Eur. Ceram. Soc. 27 (2007) 2495–2501.
[18] J.C. Han, P. Hu, X.H. Zhang, S.H. Meng, W.B. Han, Oxidation-resistant ZrB_2–SiC composites at 2200 °C, Compos Sci. Technol. 68 (2008) 799–806.
[19] S.N. Karlsdottir, J.W. Halloran, Oxidation of ZrB_2–SiC: influence of SiC content on solid and liquid oxide phase formation, J. Am. Ceram. Soc. 92 (2) (2009) 481–486.
[20] Z.Q. Cai, L. Wang, G. Yang, Dictionary of Ceramic Materials. Chemistry and Chemical Technology Press, Beijing, 2005, (in chinese).
[21] L.F. Cheng, Y.D. Xu, L.T. Zhang, X.G. Luan, Oxidation and defect control of CVD SiC coating on three dimensional C/SiC composites, Carbon 40 (2002) 2229–2234.
[22] J.S. Lian, Q.Z. Dong, Z.X. Guo, Q. Xu, J. Yang, J.D. Hu, et al., Surface oxidation kinetics of Cr film by Nd-YAG laser, Mater. Sci. Eng. A 391 (2005) 210–220.
[23] E.H. Adema, P. Heeres, Dry deposition of sulphur dioxide and ammonia on wet surfaces and the surface oxidation kinetics of bisulphite, Atmos. Environ. 29 (10) (1995) 1091–1103.
[24] H. Delalu, J.R. Vignalou, M. Elkhatib, R. Metz, Kinetics and modeling of diffusion phenomena occurring during the complete oxidation of zinc powder: influence of granulometry, temperature and relative humidity of the oxidizing fluid, Solid State Sci. 2 (2002) 229–235.
[25] S.Q. Guo, T. Mizuguchi, M. Ikegami, Y. Kagawa, Oxidation behavior of ZrB_2–$MoSi_2$–SiC composites in air at 1500 °C, Ceram. Int 37 (2011) 585–591.
[26] S.R. Levine, E.J. Opila, M.C. Halbig, J.D. Kiser, M. Singh, J.A. Salem, Evaluation of ultra-high temperature ceramics for aeropropulsion use, J. Eur. Ceram. Soc. 22 (2002) 2757–2767.
[27] S.N. Karlsdottir, J.W. Halloran, Rapid oxidation characterization of ultra-high temperature ceramics, J. Am. Ceram. Soc. 90 (10) (2007) 3233–3238.